EvaRID-50th Percentile Female Biofidelity Evaluation Assessed Against Volunteers in a Low-Speed Rear Impact

Dominic J. Isopi, Paul J. Depinet, Andrew Steinhour, Brian Loeber, Breanna Greenlees

Abstract The EvaRID Anthropomorphic Test Device (ATD) started as a 50th percentile female Computer Aided Engineering (CAE) model developed in 2012 to simulate human females in rear impacts. The design is based off the BioRID-II CAE model, a 50th percentile male ATD, but the anthropometry was adjusted to represent a female. The physical EvaRID design was updated to improve usability, performance consistency, and implement improvements learned from BioRID-II investigations. Four physical EvaRID-50F ATD's were subsequently constructed and tested for global evaluation toward potential global regulatory implementation. The biofidelity evaluation stemmed from work by Carlsson et al. (2021): a low-speed, rear impact sled test with a mean sled acceleration of 2.1g's at 10- and 15-centimeter headrest distances. Using NHTSA's BioRank quantitative analysis, the four ATD's received a good BioRank of 0.93, 1.00, 1.21, and 1.20, for an overall BioRank of 1.11. The physical EvaRID-50F is assisting with whiplash test protocol development worldwide.

Keywords ATD, EvaRID-50F, female, whiplash, biofidelity

I. INTRODUCTION

Low-speed rear impacts are widely evaluated using the BioRID-II Anthropomorphic Test Device (ATD), which represents a 50th percentile male occupant and is optimized for such loading conditions. However, this model does not represent female occupants, who constitute a substantial portion of the driving population. The EU-funded ADSEAT program addressed this limitation by advancing research toward sex-specific occupant models, resulting in the development of the EvaRID CAE model, a 50th percentile female ATD [2].

Prior research has identified the 50th percentile female as a demographic with elevated whiplash injury risk relative to smaller and larger individuals [3]. Foundational work by Carlsson et al. employed volunteer testing on a custom seat mounted to a sled system, establishing the experimental basis for EvaRID development [1,3,4]. The EvaRID v1.0 CAE model was derived by scaling the BioRID-II model according to established anthropometric factors [2]. This model was subsequently validated against volunteer response data [1,3].

The EvaRID CAE model is now widely applied by automotive manufacturers for evaluating seat performance in low-speed rear impacts. Building on this framework, Carlsson further developed the BioRID-P50F, a hybrid physical prototype incorporating components from both BioRID-II and Hybrid-III 5th percentile female ATDs, demonstrating improved sensitivity to seat performance and underscoring the need for a dedicated female rear-impact ATD [6].

In response, the process of designing, developing, and validating a production-ready physical EvaRID ATD. The present study evaluates the biofidelity of this productionized ATD, herein referred to as EvaRID-50F, through comparison with human volunteer response corridors.

II. METHODS

The study below has 2 parts: recreation of Chalmers sled, and evaluation of biofidelity of the EvaRID-50F. Note that any XYZ directions pointed out in this paper follow SAE J211 directional standards.

Dominic J. Isopi is a Senior Engineer in Farmington Hills, MI (+12487782142, disopi@humaneticsatd.com). Paul J. Depinet is a Chief Engineer in Huron, OH. Andrew Steinhour and Brian Loeber are Test Engineers in Huron, OH. Breanna Greenlees is an Engineering Manager in Farmington Hills, MI. All authors work for Humanetics Safety.

Design Highlights of EvaRID-50F

The EvaRID v1.0 CAE model was derived through direct scaling of the BioRID-II CAE model, thereby preserving its underlying design intent and performance characteristics; comprehensive design details of the BioRID-II are provided in [5]. During productionization for the EvaRID-50F, all performance-critical components of the EvaRID v1.0 CAE model were retained in the physical EvaRID-50F, ensuring consistency between virtual and physical implementations. The overall geometry, including vertebral architecture, bumper configuration, and spring-damper system, remained unchanged, with only minor modifications introduced. Specifically, the VIVA+ human body model was used to refine the silicone torso jacket and pelvis flesh geometry, improving biofidelity and smoothing transitions between anatomical regions [7]. Additionally, the Occipital Condyle (OC) interface design used in the BioRID-II was eliminated. In its place, a redesigned head assembly was rigidly mounted to the C0 plate, removing the compliant bumper interface and thereby reducing variability associated with skull–neck interaction.

All other modifications were limited to improvements in usability, repeatability, and reproducibility, without altering fundamental performance behavior. Segment mass distributions were strictly maintained according to established specifications [3], and the direct geometric correspondence with the CAE model supports the expectation of comparable kinematic response between the physical EvaRID-50F and its virtual counterpart. The finalized ATD incorporates up to 48 instrumentation channels, of which 36 are utilized for biofidelity evaluation. See Table 4 in the Appendix for details.

Recreation of Chalmers Sled at Humanetics

The biofidelity evaluation of the EvaRID-50F utilizes a seat custom-designed by Chalmers University for low-speed rear impact testing, hereafter referred to as the Chalmers Seat [4]. This seat served as the experimental platform for all prior Chalmers studies, including both volunteer testing and BioRID-P50F evaluations. To enable efficient testing and maintain experimental consistency, a geometrically and mechanically representative replica of the Chalmers Seat was developed.

The original Chalmers Seat was temporarily integrated with the Humanetics E-Liner FLEX ZERT system and instrumented using a certified BioRID-II, subjected to the volunteer-derived sled pulse defined in [1] (Figure 1). Following initial validation, the seat was disassembled to characterize its deformable components, including headrest foams and panel spring systems, then reassembled, revalidated, and returned to Chalmers University. A replica seat was subsequently fabricated using machined and commercially sourced components matched to the original design.

The replicated seat was evaluated using the same BioRID-II configuration and sled pulse conditions as the original system [1], ensuring direct comparability between test setups. Performance equivalence was assessed through two Chalmers Seat tests and three replica seat tests, from which a ±10% corridor was established based on the Chalmers baseline to validate the biofidelity of the replica seat. A head restraint distance of 15 cm was selected to maximize seat contribution to head and neck kinematics prior to headrest contact.

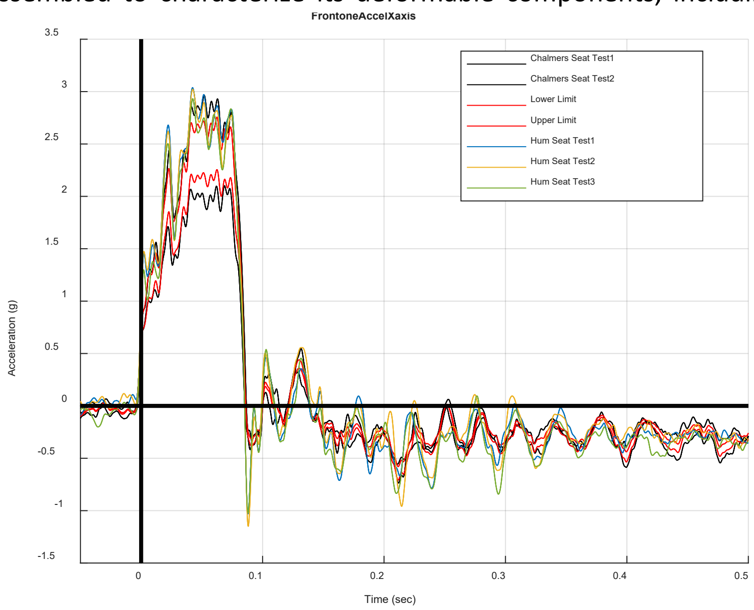

Figure 1 - The Sled Acceleration of all five Seat Validation tests with upper and lower limits. Red lines are the Chalmers Seat data or the limits created from them.

Biofidelity Evaluation of EvaRID-50F

The biofidelity evaluation of the EvaRID-50F was conducted in accordance with the methodology defined in [1]. The evaluation utilized the replicated Chalmers Seat described in the preceding section. The seat was mounted to an E-Liner FLEX ZERT sled system, which applied the acceleration pulse shown in Figure 1 under conditions consistent with the seat validation tests. The pulse exhibited a peak acceleration of approximately 2.9 g with a duration of ~100 ms, and the corresponding sled velocity reached a peak of approximately 1.8 m/s. The ATD was positioned according to a standardized procedure described below.

1. Verify dummy joints are set to 1-2g's.
2. Make sure dummy is centered left-to-right about the chair / head rest.
3. Push on knees so pelvis and thighs are down on chair base and the dummy's lower back is against the bottom chair padding.
4. Place the shoes with toes pointing up flat against the angled foot plate such that the outside edge of each shoe is flush with the gussets. This translates to about a 4.5" apart measured from the inside edge to inside edge. Lift / bend knees as necessary.
5. Space the knees ~8.5" apart from center-to-center.
6. Rest the hands on the top of the knee flesh with palms down and elbows angled outward.
7. Push the upper thorax back into the chair and repeat Steps 3-7 above as necessary.
8. Adjust the ATD tilt sensors according to below:
    a. Head: X-axis: 0° ± 0.5°; Y-axis: 0° ± 1°
    b. Pelvis: X-axis: 0° ± 0.5°; Y-axis: 20° ± 3°

The experimental protocol defined in [1] incorporates two head restraint distances, 10 cm and 15 cm. Following ATD positioning, the head restraint distance was adjusted by varying the number of headrest foam layers. High-speed tracking markers were applied to the Pelvis Flag, T1 Flag, Head CG, and a secondary head location to capture both translational and rotational kinematics. An H-point target tool was additionally employed to provide a redundant measurement of Pelvis X displacement. Instrumentation channels used for biofidelity assessment are summarized in Table 4 of the Appendix. High-speed video data was acquired at 1000 frames per second, while the data acquisition system (DAS) operated at a sampling rate of 20 kHz. Four EvaRID-50F ATDs were constructed and evaluated, with each ATD subjected to three repeated tests at both head restraint distances, yielding a total of 24 tests.

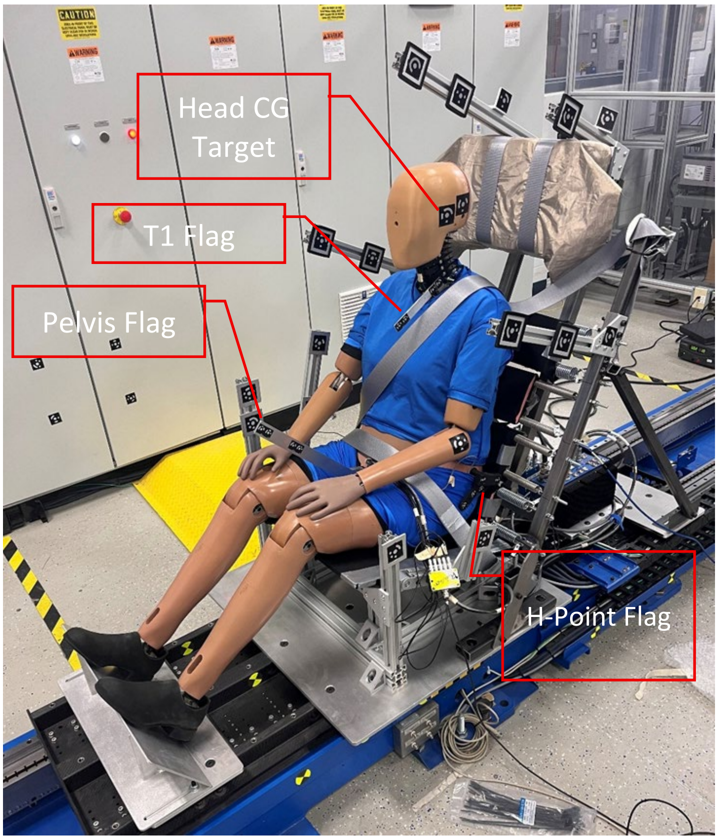

Figure 2 - A picture of the biofidelity setup at Humanetics for testing the EvaRID-50F. Note the targets on the ATD for high-speed video tracking.

Initially, the Pelvis X displacement was not recorded due to the focus of high-speed imaging on the head and neck regions, but this omission was subsequently corrected for two of the four evaluated ATDs. Moreover, measurement methodologies differed between volunteer and ATD datasets, including those for the BioRID-P50F. In volunteer testing, the trochanter major was palpated and its initial position recorded prior to testing [1], after which two high-speed markers were placed along the femur and tracked to extrapolate trochanter X displacement [1]. In contrast, ATD measurements utilized either the Pelvis Flag or H-point to quantify Pelvis X displacement [6].

The U.S. National Highway Traffic Safety Administration (NHTSA) developed the BioRank methodology as an objective framework for evaluating ATD biofidelity [8,9]. The most recent implementation of BioRank [9] was applied in this study, using the minimum dummy cumulative absolute difference over cadaver cumulative standard deviation (DCAD/CCSD) as the time-history alignment criterion. No phase shifts were applied, as curve alignment was inherently consistent and BioRank values remained unchanged with shifting. The analyzed parameters are listed in Table 4 of the Appendix, and BioRank quality categories are defined in Table 1.

Table 1

BioRank Score and Biofidelity Category Summary				
BioRank Scores	BRS ≤ 1.0	1.0 < BRS ≤ 2.0	2.0 < BRS ≤ 3.0	BRS > 3.0
Biofidelity	Excellent	Good	Marginal	Poor

Volunteer datasets included evaluation durations of 300 ms and 500 ms; however, all parameters were truncated to 300 ms in this study for consistency and prioritizing the impact phase. Head-to-headrest contact is completed by approximately 180 ms, after which rebound behavior dominates and increasingly influences BioRank outcomes. Additionally, extended evaluation windows introduce variability due to chaotic rebound motion, artificially improving BioRank scores.

BioRank analysis is typically organized by anatomical regions, i.e. head, neck, pelvis, etc. However, the organization is complicated by Head Relative to T1 Displacement and Head Relative to T1 Angle spanning multiple regions. Pelvis X Displacement data was also incomplete. Accordingly, all parameters were weighted equally to simplify evaluation. Left and right T1 acceleration BioRank values were averaged to produce a single representative metric.

III. RESULTS

Seat Validation Performance

During the replicated seat validation, four key parameters were selected to assess the biofidelity of the replicated seat for EvaRID-50F: Head X Displacement, Head Angular Rotation, T1 Acceleration, and T1 Rotation. Figure 3–6 compare Chalmers Seat responses (dark red curves), the corresponding ±10% corridor derived from their mean response (light red curves), and replica seat responses (multi-colored curves). Across all evaluated parameters, the replica seat demonstrates strong agreement with the Chalmers Seat, with response traces consistently falling within or closely bounding the established corridor. The sole deviation is observed in replica seat Test 2 for T1 Rotation, where an abrupt decrease at approximately 0.09 s is followed by a rapid return to nominal response behavior at 0.13 s, indicating a localized anomaly rather than a systematic discrepancy.

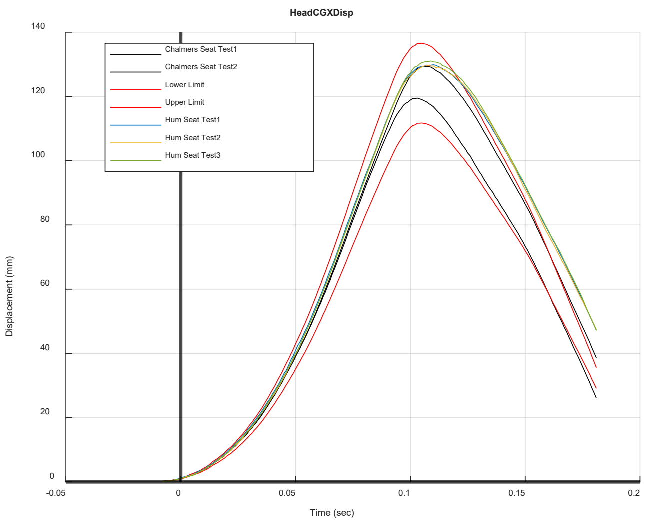

Figure 3 - The Head CG X Displacement of the BioRID-II evaluated in both the Chalmers Seat with upper and lower limits and the Replica Seat.

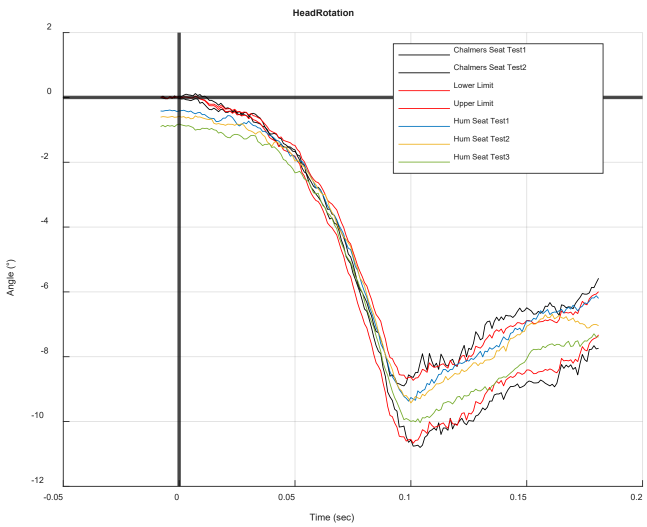

Figure 4 - The Head Angle of the BioRID-II evaluated in both the Chalmers Seat with upper and lower limits and the Replica Seat.

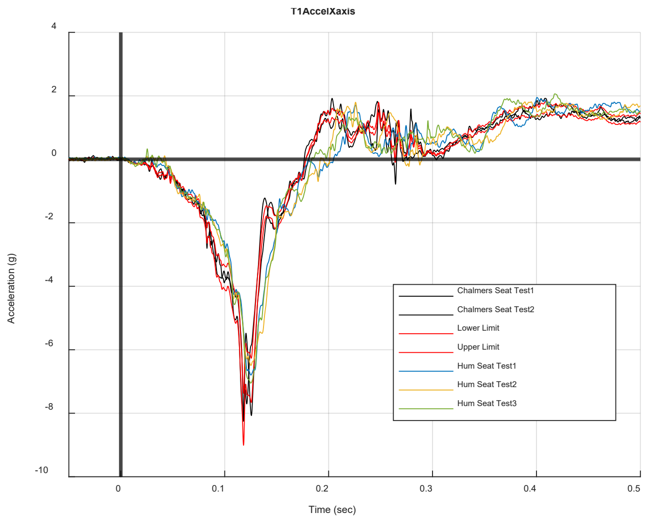

Figure 5 - The T1 X Acceleration of the BioRID-II evaluated in both the Chalmers Seat with upper and lower limits and the Replica Seat.

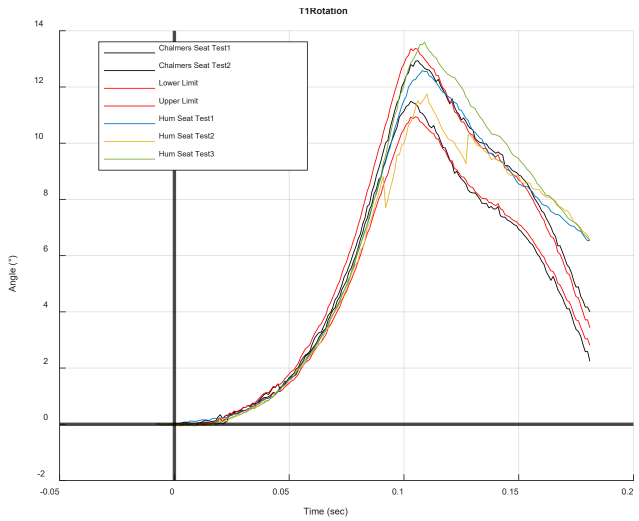

Figure 6 - The T1 Angle of the BioRID-II evaluated in both the Chalmers Seat with upper and lower limits and the Replica Seat.

EvaRID-50F Biofidelity

For clarity, a single test from the three conducted per ATD is presented in each plot, with the selected tests chosen at random. The BioRank range is indicated in all plots by a green shaded region. Where available, Carlsson et al. data extending beyond 300 ms are also included [1]. Beyond 300 ms, the volunteer corridors widen substantially, reflecting increased variability in the response data [1].

15 cm Headrest Distance

The EvaRID-50F demonstrates increased Head X Displacement relative to volunteer corridors, while exhibiting comparable or slightly reduced T1 X Displacement. Between 100 ms and 225 ms, both Head and T1 Angular Displacements are consistently lower than volunteer responses. The EvaRID-50F Head and T1 Angular Displacement both are lower than the volunteer data. Two methods were employed to evaluate Head-to-T1 relative motion: direct calculation from high-speed video (TEMA) and derivation via subtraction of Head and T1 Angular Displacements, calculated from the integration of the angular velocities. While both methods yield similar results during the early response phase (0–175 ms), the subtraction-based method aligns more closely with volunteer data from 175 ms to 300 ms, whereas the high-speed measurement provides improved agreement beyond 300 ms. Minimal inter-ATD variability is observed in high-speed video channels, with consistent curve shapes and no discernible performance differences between units.

Head X Acceleration exhibits a significantly higher peak magnitude than the volunteer corridor, which is characterized by a more gradual rise. Left and right T1 accelerations in both X and Z directions show consistent agreement across tests. However, T1 X Acceleration displays a two-peak response in the EvaRID-50F, in contrast to the single-peak profile observed in volunteer data, with the second peak exceeding both the first peak and the volunteer maximum. A similar trend is observed in T1 Z Acceleration, where the first peak closely matches the volunteer levels and the second peak exceeds them. The timing of the second T1 X Acceleration peak corresponds to a polarity reversal in T1 Z Acceleration at approximately 135 ms, coinciding with head-to-headrest contact occurring between 119 ms and 129 ms, suggesting a headrest-driven, loading mechanism transmitted through the head. Pelvis X Displacement data were not initially recorded for all ATDs, resulting in incomplete datasets for two of the four evaluated units; consequently, multiple test repetitions are presented for those cases. Two measurement approaches, the pelvis flag and H-point, produced nearly identical results, indicating measurement method independence within the ATD. Despite this consistency, the EvaRID-50F underpredicts Pelvis X Displacement by approximately 30 mm relative to volunteer data and fails to replicate the post-200 ms oscillatory response, instead exhibiting a plateau. Aside from Pelvis X Displacement, the EvaRID-50F demonstrates strong agreement with the volunteer response corridors, with overall curve shapes aligning well with the reference data [1].

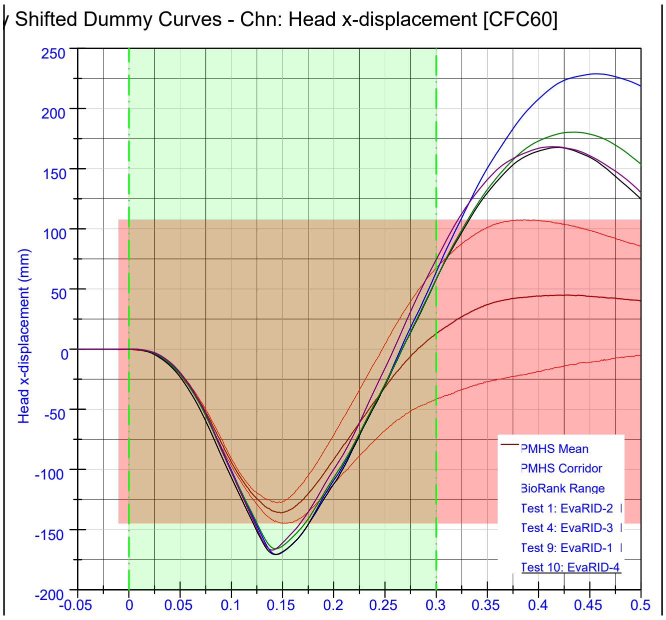

Figure 7 - The Head X Displacement for the EvaRID-50F compared against the volunteer corridor from [1] at 15cm headrest distance. Note only one test of each ATD number is shown.

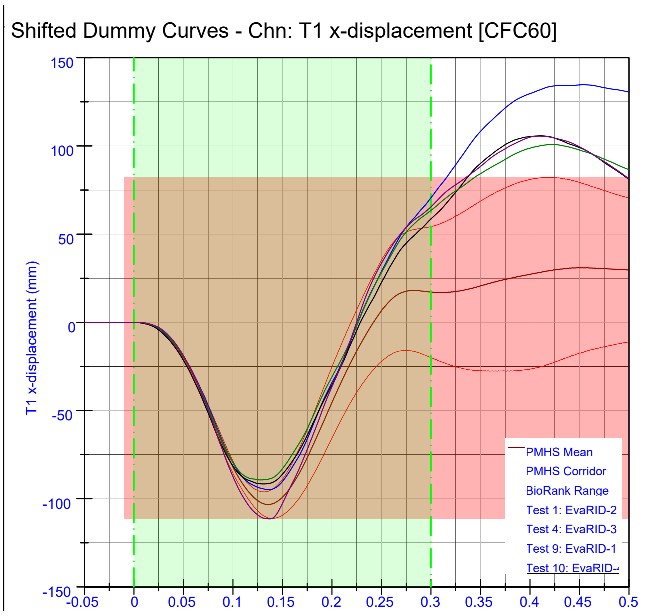

Figure 8 - The T1 X Displacement for the EvaRID-50F compared against the volunteer corridor from [1] at 15cm headrest distance. Note only one test of each ATD number is shown.

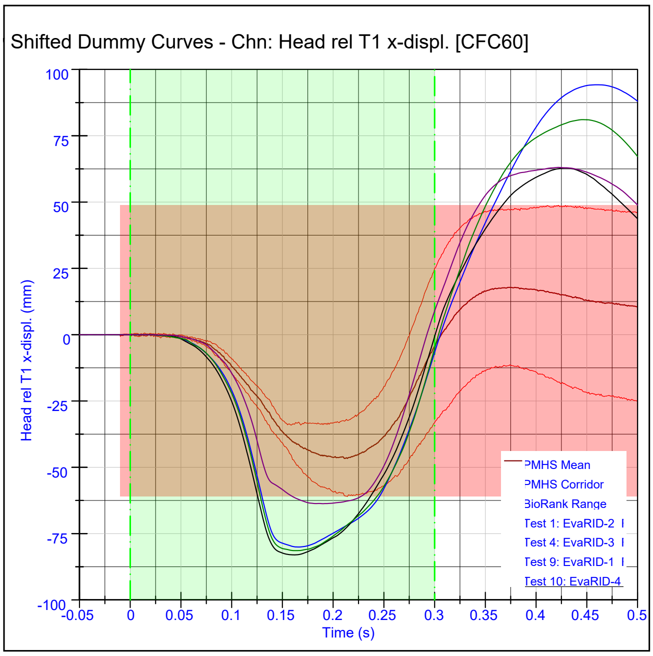

Figure 9 - The Head Relative to T1 X Displacement for the EvaRID-50F compared against the volunteer corridor from [1] at 15cm headrest distance. Note only one test of each ATD number is shown.

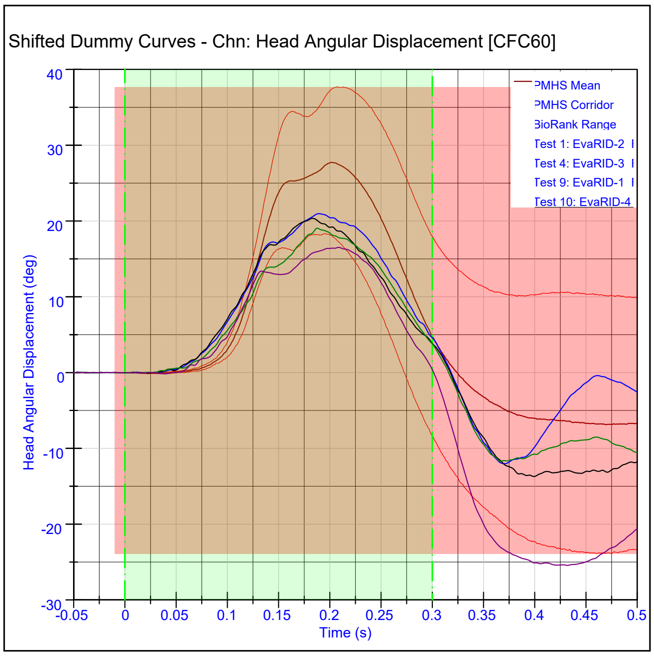

Figure 10 - The Head Angular Displacement for the EvaRID-50F compared against the volunteer corridor from [1] at 15cm headrest distance. Note only one test of each ATD number is shown.

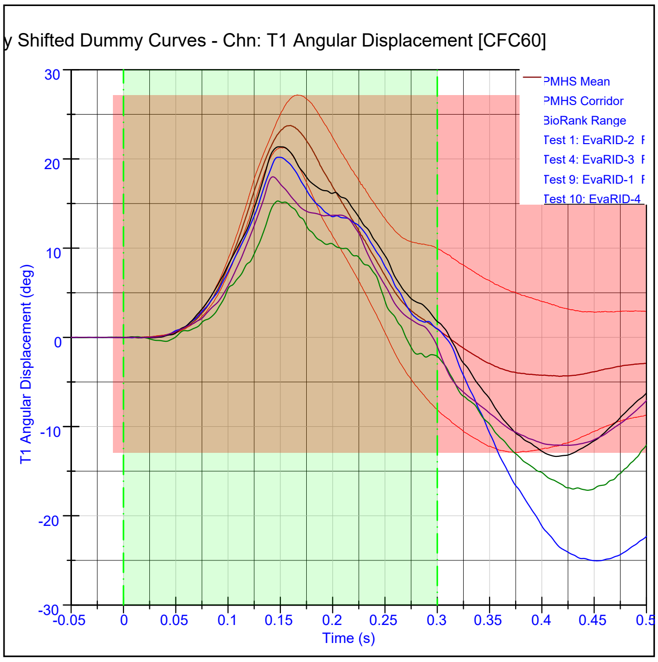

Figure 11 - The T1 Angular Displacement for the EvaRID-50F compared against the volunteer corridor from [1] at 15cm headrest distance. Note only one test of each ATD number is shown.

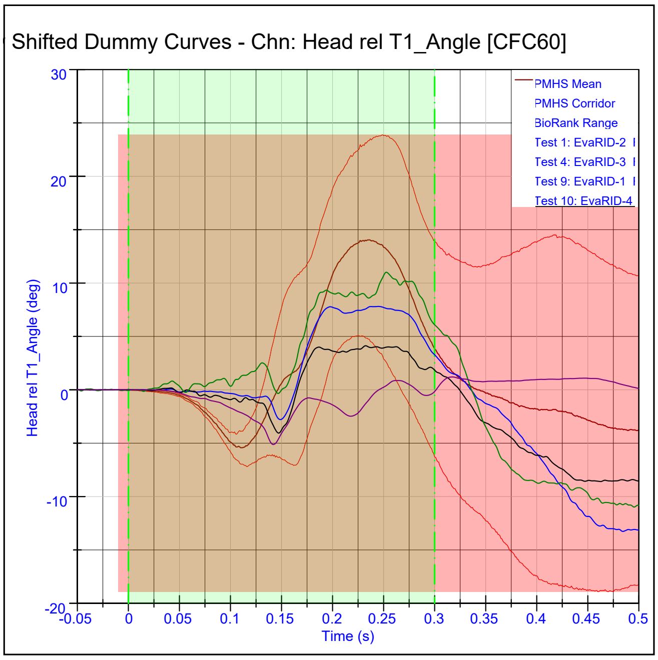

Figure 12 - The Head Relative to T1 Angular as measured by the high-speed camera for the EvaRID-50F compared against the volunteer corridor from [1] at 15cm headrest distance. Note only one test of each ATD number is shown.

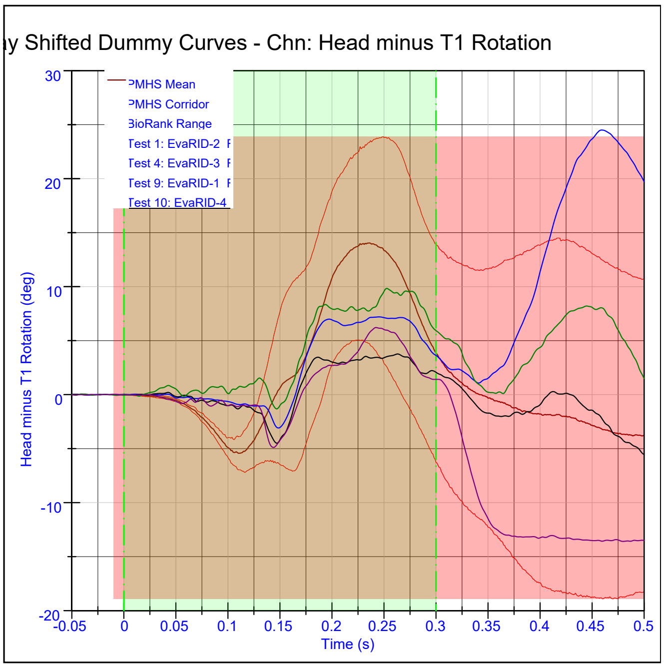

Figure 13 - The Head Minus T1 Rotation for the EvaRID-50F compared against the volunteer corridor from [1] at 15cm headrest distance. Note only one test of each ATD number is shown.

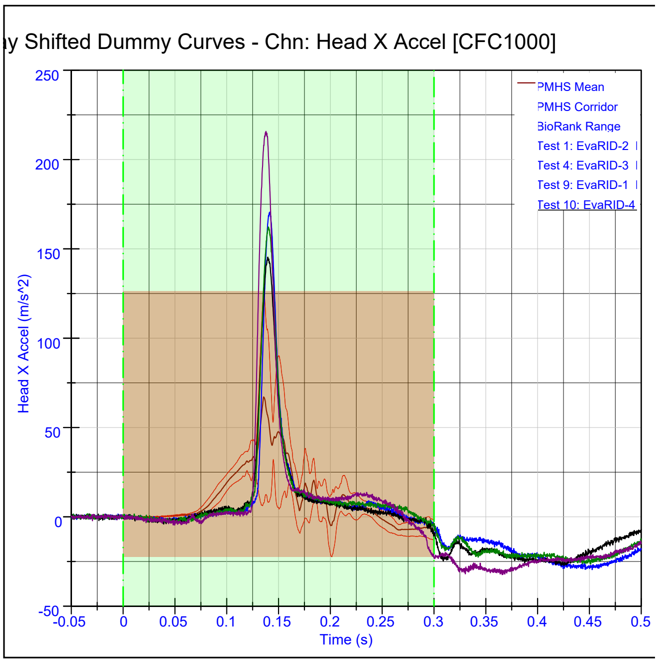

Figure 14 - The Head X Acceleration for the EvaRID-50F compared against the volunteer corridor from [1] at 15cm headrest distance. Note only one test of each ATD number is shown.

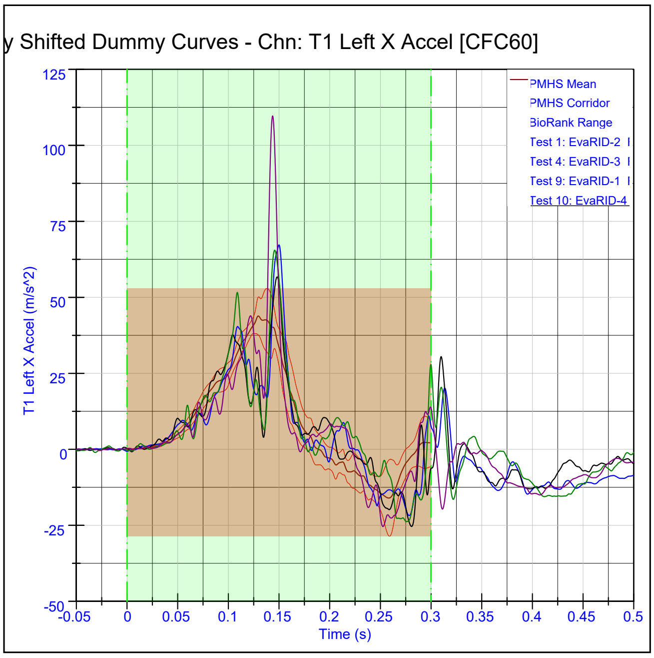

Figure 15 - The T1 Left X Acceleration for the EvaRID-50F compared against the volunteer corridor from [1] at 15cm headrest distance. Note only one test of each ATD number is shown.

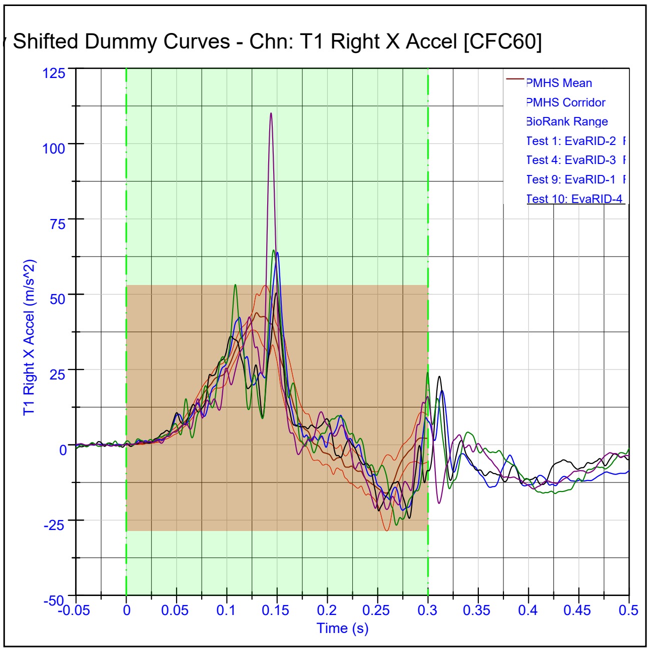

Figure 16 - The T1 Right X Acceleration for the EvaRID-50F compared against the volunteer corridor from [1] at 15cm headrest distance. Note only one test of each ATD number is shown.

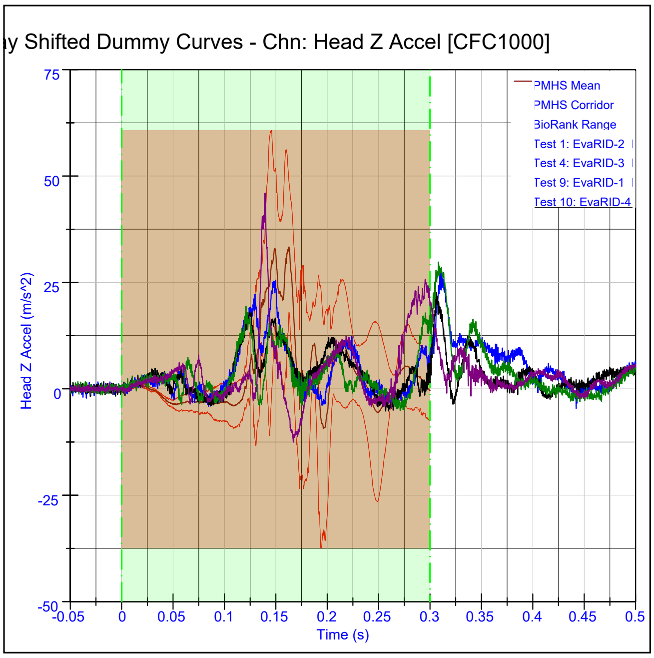

Figure 17 - The Head Z Acceleration for the EvaRID-50F compared against the volunteer corridor from [1] at 15cm headrest distance. Note only one test of each ATD number is shown.

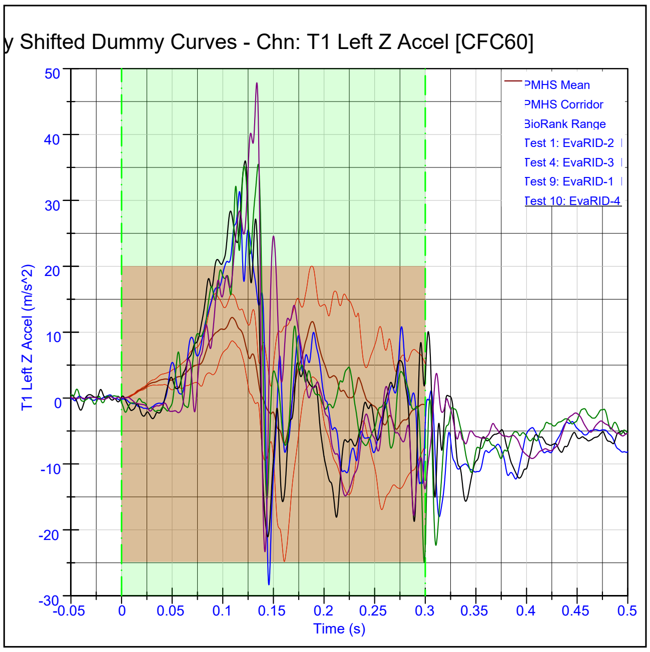

Figure 18 - The T1 Left Z Acceleration for the EvaRID-50F compared against the volunteer corridor from [1] at 15cm headrest distance. Note only one test of each ATD number is shown.

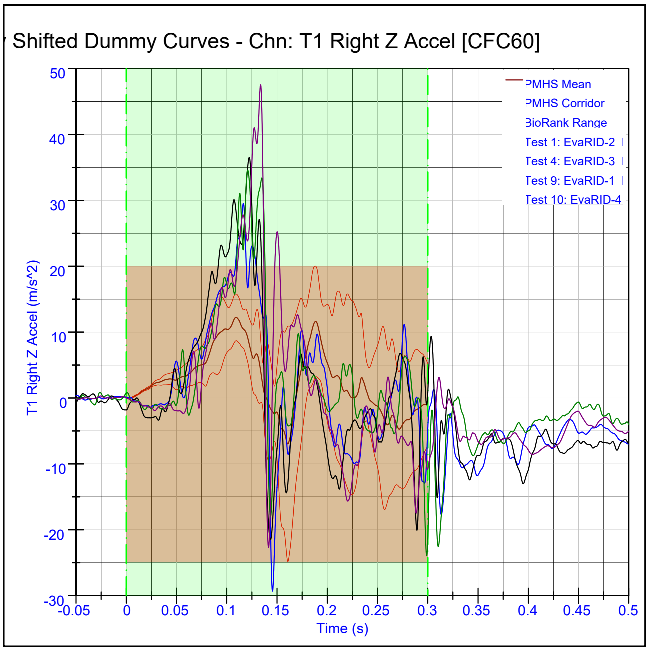

Figure 19 - The T1 Right Z Acceleration for the EvaRID-50F compared against the volunteer corridor from [1] at 15cm headrest distance. Note only one test of each ATD number is shown.

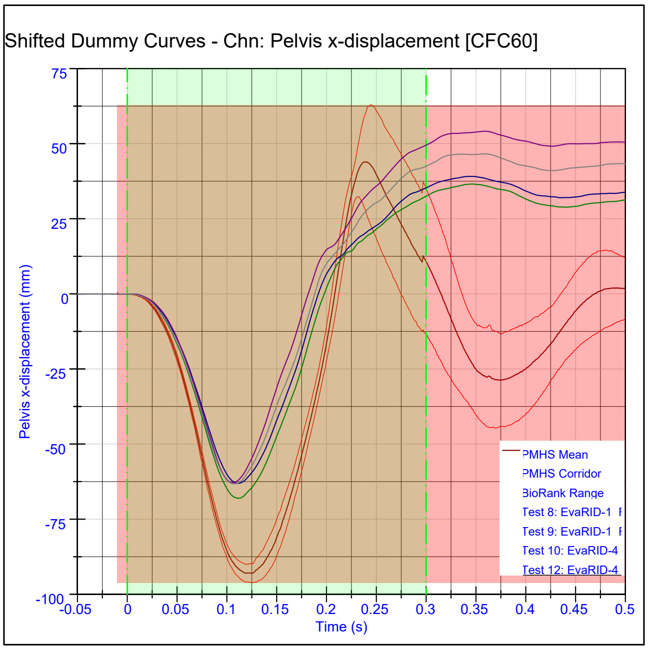

Figure 20 - The Pelvis X displacement measured by the pelvis flag for the EvaRID-50F compared against the volunteer corridor from [1] at 15cm headrest distance. Note only one test of each ATD number is shown.

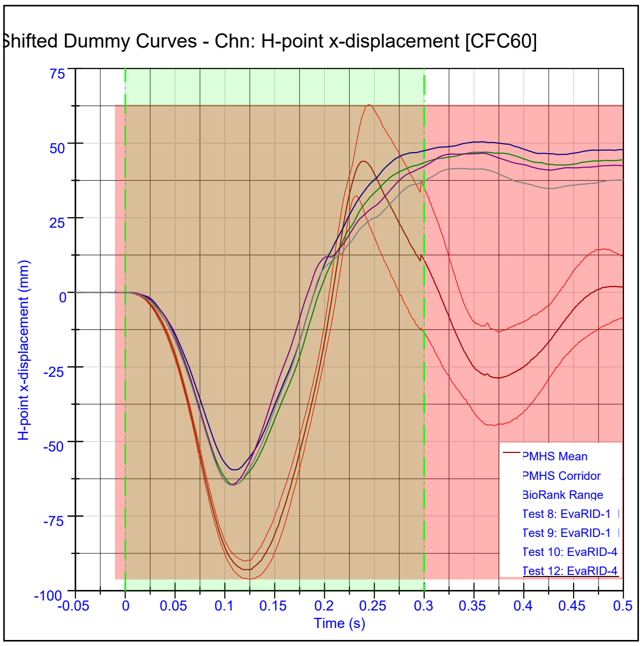

Figure 21 - The H-Point Pelvis Displacement measured by the H-point tool for the EvaRID-50F compared against the volunteer corridor from [1] at 15cm headrest distance. Note only one test of each ATD number is shown.

10 cm Headrest Distance

The 10 cm head restraint distance tests exhibit trends consistent with those observed at 15 cm. Head X Displacement shows a slightly higher peak, while T1 X Displacement is comparatively lower, resulting in a modest increase in relative displacement that remains within the established corridor. Head Angular Displacement closely follows the corridor mean, whereas T1 Angular Displacement is consistently underpredicted across all ATDs. Notably, EvaRID #2 (Test 2, Test 1 and 3 are not plotted) exhibits an elevated post-300 ms peak in T1 angular displacement relative to both volunteer data and other ATDs, suggesting an ATD-specific anomaly. Relative Head-to-T1 motion demonstrates similar methodological trends across both calculation approaches, with strong agreement in the early phase, improved correlation with the subtraction method at mid-time, and notable agreement with high-speed video measurements at later times. Head X and Z Accelerations display a single-peak response, in contrast to the dual-peak profile observed in volunteer data. T1 Accelerations in the X and Z directions are consistent, with T1 X Acceleration largely remaining within the corridor. However, T1 Z Acceleration deviates from the volunteer trend, remaining positive between 0–175 ms before transitioning negative, whereas volunteer responses return to near-zero levels. Pelvis X Displacement follows trends consistent with the 15 cm condition, with the EvaRID-50F underpredicting displacement by approximately 30 mm and failing to replicate the oscillatory behavior observed in volunteer data beyond 200 ms. Head-to-headrest contact occurs between 95 ms and 110 ms. Aside from discrepancies in Pelvis X Displacement and T1 Z Acceleration, the EvaRID-50F demonstrates overall agreement with the volunteer response corridors defined by Carlsson et al. [1].

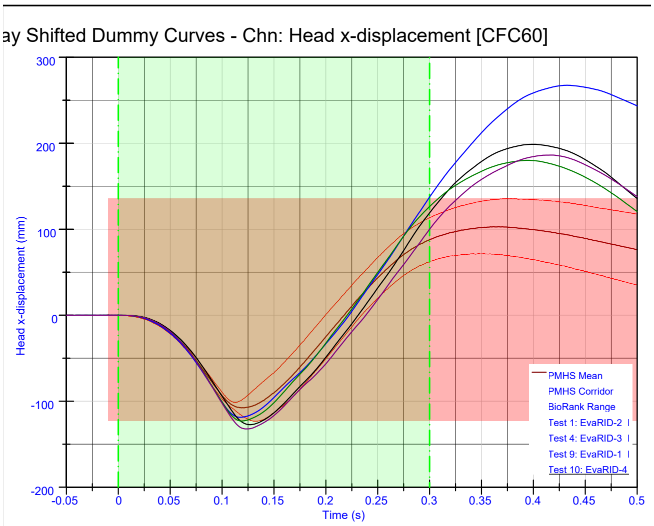

Figure 22 – The Head X Displacement for the EvaRID-50F compared against the volunteer corridor from [1] at 10cm headrest distance. Note only one test of each ATD number is shown.

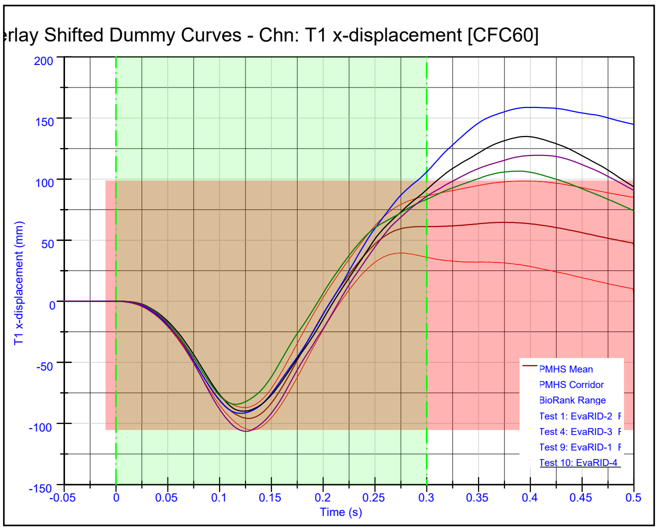

Figure 23 – The T1 X Displacement for the EvaRID-50F compared against the volunteer corridor from [1] at 10cm headrest distance. Note only one test of each ATD number is shown.

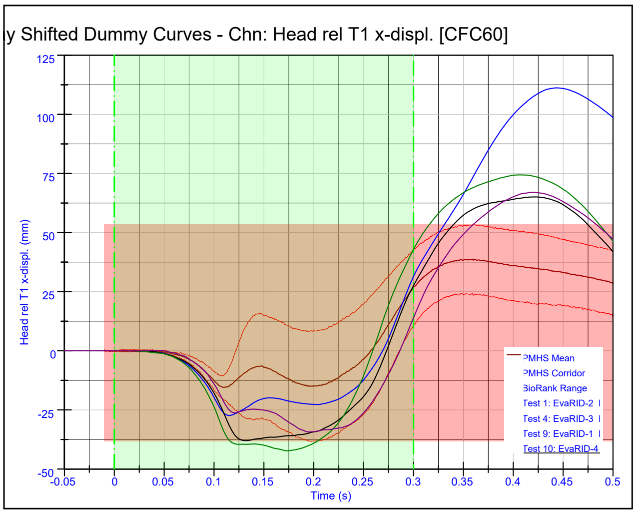

Figure 24 – The Head Relative to T1 X Displacement for the EvaRID-50F compared against the volunteer corridor from [1] at 10cm headrest distance. Note only one test of each ATD number is shown.

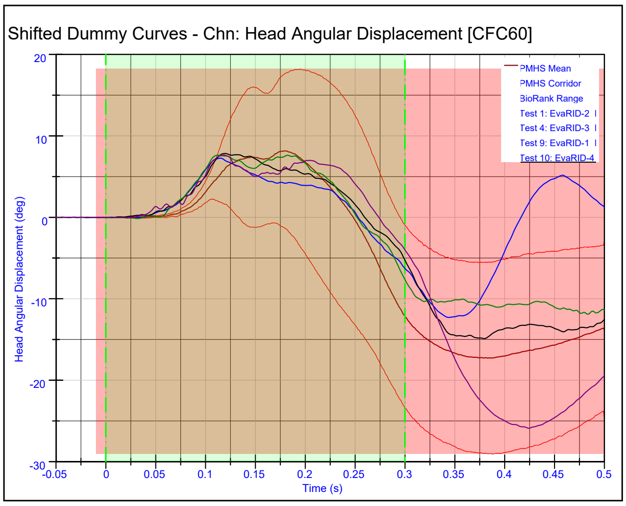

Figure 25 – The Head Angular Displacement for the EvaRID-50F compared against the volunteer corridor from [1] at 10cm headrest distance. Note only one test of each ATD number is shown.

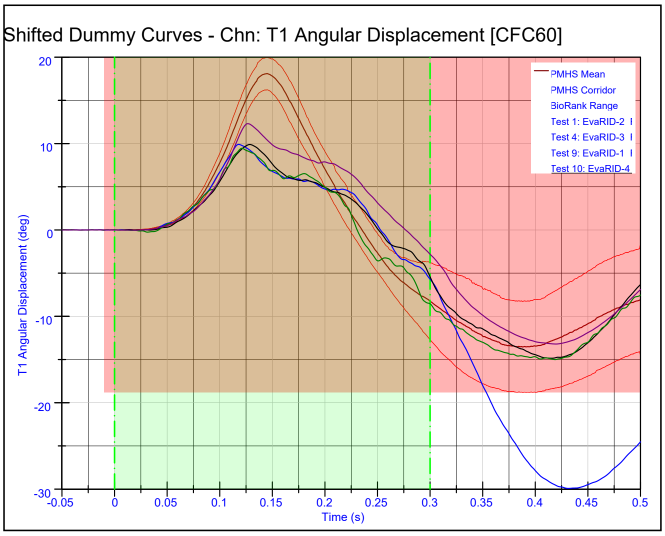

Figure 26 – The T1 Angular Displacement for the EvaRID-50F compared against the volunteer corridor from [1] at 10cm headrest distance. Note only one test of each ATD number is shown.

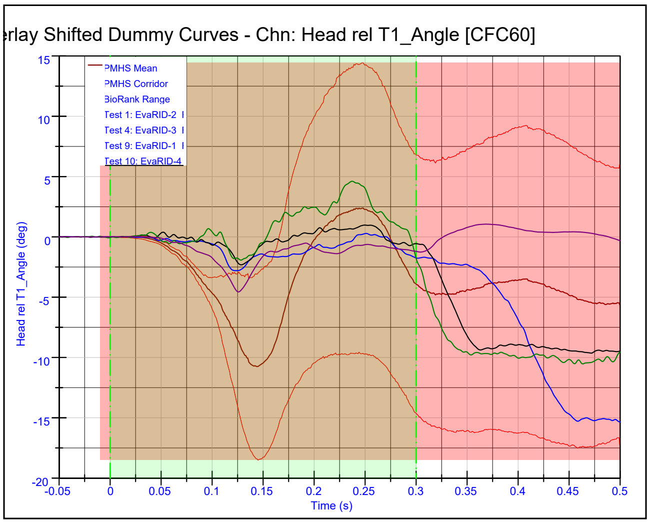

Figure 27 – The Head Relative to T1 Angular as measured by the high-speed camera for the EvaRID-50F compared against the volunteer corridor from [1] at 10cm headrest distance. Note only one test of each ATD number is shown.

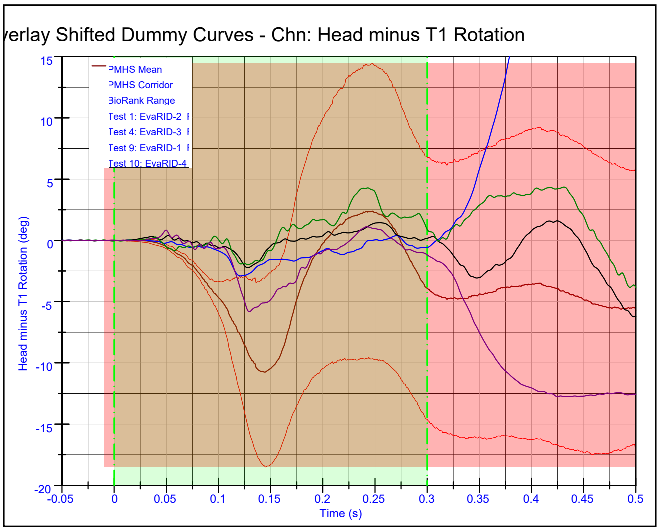

Figure 28 – The Head Minus T1 Rotation for the EvaRID-50F compared against the volunteer corridor from [1] at 10cm headrest distance. Note only one test of each ATD number is shown.

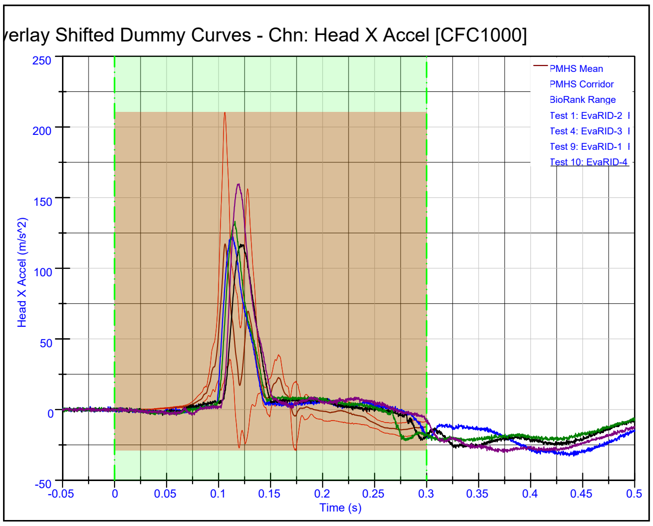

Figure 29 – The Head X Acceleration for the EvaRID-50F compared against the volunteer corridor from [1] at 10cm headrest distance. Note only one test of each ATD number is shown.

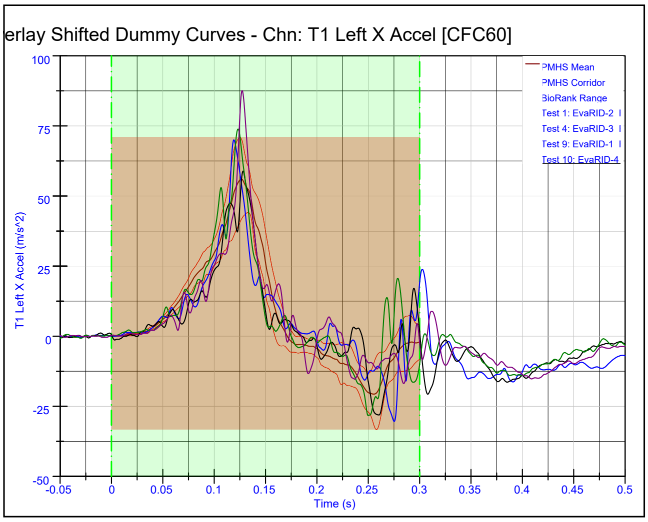

Figure 30 – The T1 Left X Acceleration for the EvaRID-50F compared against the volunteer corridor from [1] at 10cm headrest distance. Note only one test of each ATD number is shown.

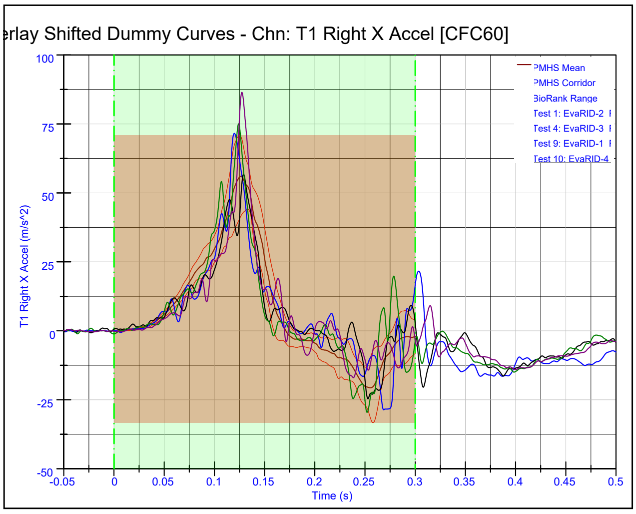

Figure 31 – The T1 Right X Acceleration for the EvaRID-50F compared against the volunteer corridor from [1] at 10cm headrest distance. Note only one test of each ATD number is shown.

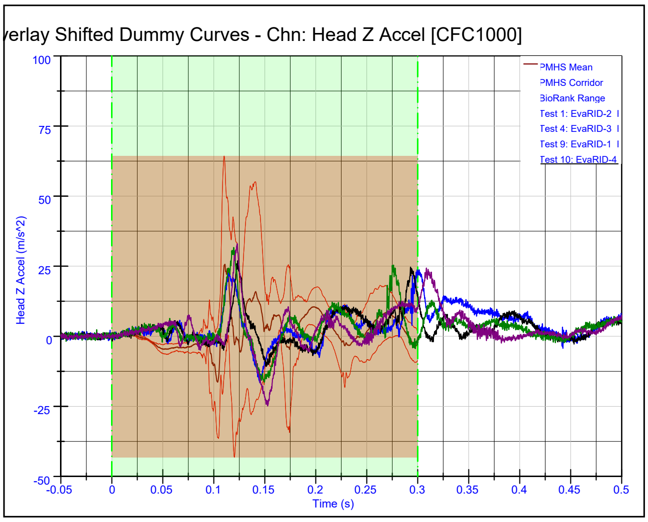

Figure 32 – The Head Z Acceleration for the EvaRID-50F compared against the volunteer corridor from [1] at 10cm headrest distance. Note only one test of each ATD number is shown.

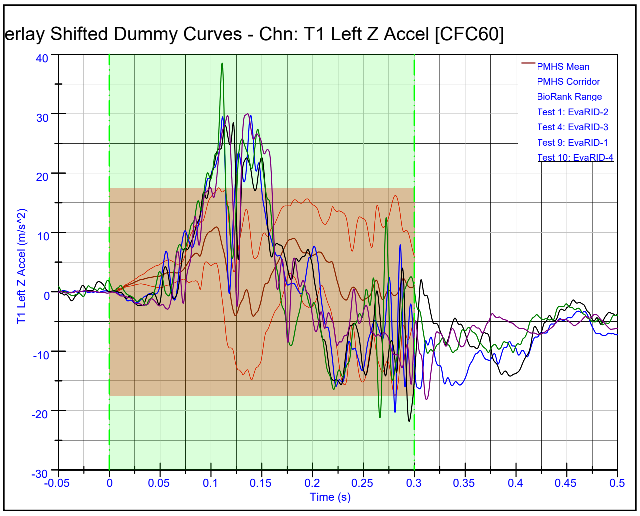

Figure 33 – The T1 Left Z Acceleration for the EvaRID-50F compared against the volunteer corridor from [1] at 10cm headrest distance. Note only one test of each ATD number is shown.

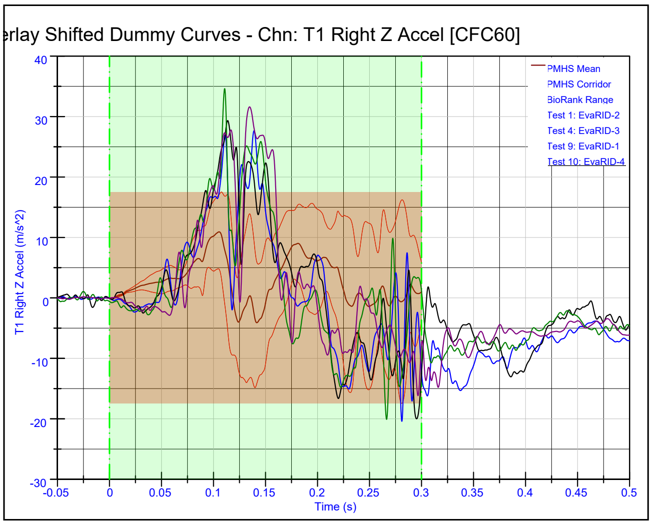

Figure 34 – The T1 Right Z Acceleration for the EvaRID-50F compared against the volunteer corridor from [1] at 10cm headrest distance. Note only one test of each ATD number is shown.

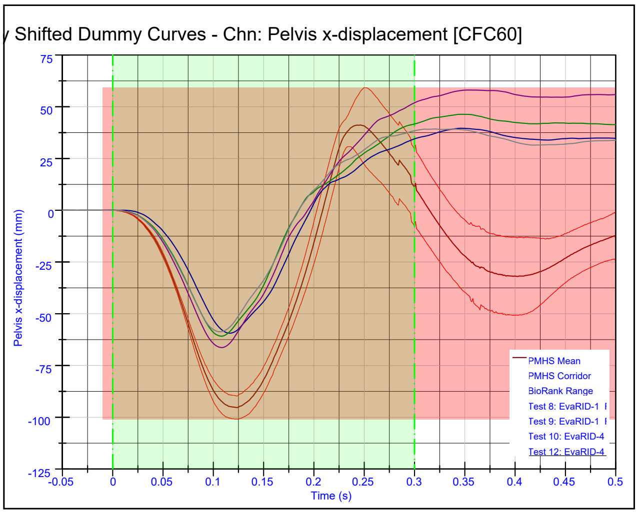

Figure 35 – The Pelvis X displacement measured by the pelvis flag for the EvaRID-50F compared against the volunteer corridor from [1] at 10cm headrest distance. Note only one test of each ATD number is shown.

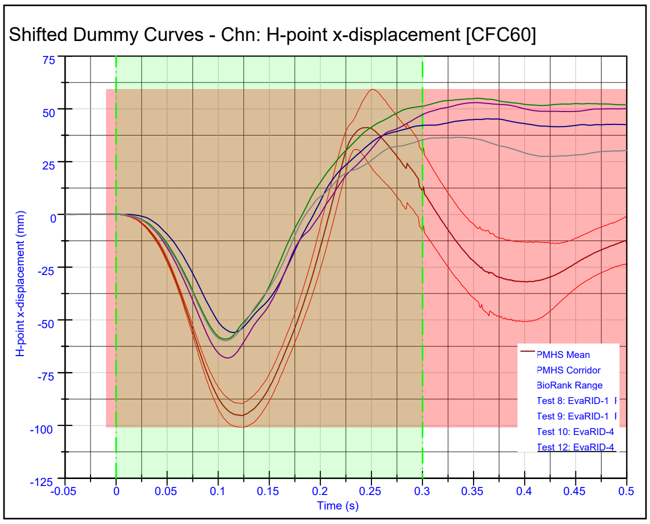

Figure 36 – The H-Point Pelvis Displacement measured by the H-point tool for the EvaRID-50F compared against the volunteer corridor from [1] at 10cm headrest distance. Note only one test of each ATD number is shown.

BioRank Calculation

The EvaRID-50F BioRank data is shown below in Table 2 and Table 3 with detailed test-level values provided in Appendix B. The overall BioRank is 1.11 when Pelvis X Displacement is included and 0.97 when excluded, corresponding to Good and Excellent biofidelity classifications, respectively. If Pelvis X Displacement data had been available for EvaRID #2 and #3, the overall BioRank is expected to increase to approximately 1.20 for the 15 cm condition, while remaining within the “Good” category. Performance improved under the 10 cm head restraint condition relative to the 15 cm condition, with all parameters except T1 Angular Displacement exhibiting lower BioRank values. Across repeated tests, all parameters, excluding Pelvis X Displacement, remained below 2.0, indicating strong overall ATD performance. Notably, EvaRID #1 and #4 exhibited higher BioRank values than EvaRID #2 and #3; these tests were conducted approximately six months later, and EvaRID #1 was subsequently retested to assess consistency. Overall, the EvaRID-50F demonstrates good agreement with volunteer response corridors, supporting its validity for representing a 50th percentile female in low-speed rear impact evaluations.

Table 2 *- Summary of the BioRank Scores from the 15cm headrest distance tests.*

Parameter	EvaRID #2	EvaRID #3	EvaRID #1	EvaRID #4	Parameter BioRank
Head x-Displacement	0.87	0.92	0.74	0.89	0.86
T1 x-Displacement	0.86	1.02	1.05	0.86	0.95
Head rel T1 x-Displ.	1.81	1.89	1.94	1.03	1.67
Head Angular Displacement	0.55	0.71	0.77	0.91	0.74
T1 Angular Displacement	0.47	0.59	1.03	0.75	0.71
Linkage Angle	0.51	0.63	0.57	0.92	0.66
Head X Accel	1.26	1.10	1.24	1.69	1.32
T1 X Acceleration	1.55	1.49	1.80	1.47	1.58
Head Z Accel	0.56	0.59	0.66	0.76	0.64
T1 Z Acceleration	0.89	1.07	0.96	1.24	1.04
Pelvis/H-Point X Displacement			2.49	2.73	2.61
ATD BioRank	0.93	1.00	1.21	1.20	1.16
ATD BioRank without Pelvis X Displacement	0.93	1.00	1.08	1.05	1.02

Table 3 *- Summary of the BioRank Scores from the 10cm headrest distance tests.*

Parameter	EvaRID #2	EvaRID #3	EvaRID#1	EvaRID #4	Parameter BioRank
Head x-Displacement	0.53	0.87	0.71	1.05	0.79
T1 x-Displacement	0.88	0.56	1.01	0.64	0.77
Head rel T1 x-Displ.	0.54	0.95	1.03	0.87	0.85
Head Angular Displacement	0.28	0.24	0.22	0.34	0.27
T1 Angular Displacement	1.81	1.86	1.72	1.91	1.82
Linkage Angle	0.42	0.44	0.58	0.38	0.45
Head X Accel	0.84	1.10	1.14	1.40	1.12
T1 X Acceleration	1.09	0.96	1.04	1.05	1.03
Head Z Accel	0.67	0.73	0.71	0.79	0.73
T1 Z Acceleration	1.11	1.26	1.23	1.29	1.22
Pelvis/H-Point X Displacement			2.76	2.52	2.64
ATD BioRank	0.82	0.90	1.10	1.11	1.06
ATD BioRank without Pelvis X Displacement	0.82	0.90	0.94	0.97	0.91

IV. DISCUSSION

Seat Verification Performance

Based on the data collected, the Humanetics Seat demonstrates equivalent performance to the Chalmers Seat and is suitable for future EvaRID-50F biofidelity evaluations. It may also serve as a viable platform for future BioRID-II biofidelity assessments. A localized anomaly was observed in replicated seat Test 2, where T1 angular displacement exhibited abrupt discontinuities; this deviation is attributed to high-speed video tracking error rather than structural seat behavior. When this artifact is disregarded, the response aligns closely with the remaining Humanetics Seat tests, reinforcing overall consistency. Due to the Pelvis X-Displacement discrepancy in the EvaRID-50F evaluation, future verification studies of rear impact seats should include this parameter.

EvaRID-50F Biofidelity

Many response trends observed in the 15 cm head restraint condition are consistently reproduced in the 10 cm configuration. Notably, Head Displacement exceeds T1 Displacement, resulting in increased relative motion between these anatomical landmarks. In both conditions, T1 Angular Displacement is underpredicted, indicating that the spinal response of the ATD is likely too stiff relative to volunteer data. While this stiffness may be reduced through modification of the bumper system, doing so would likely require adjustments to intervertebral spacing, which presents significant practical challenges. More work is suggested to investigate the differences. T1 Acceleration responses in the 15 cm condition exhibit behavior that deviates from volunteer data, with inconsistencies in both peak magnitude and temporal alignment. The occurrence of multiple peaks, combined with poor temporal correlation, suggests an alternate loading mechanism not present in volunteer testing. Given that several of these peaks occur after head-to-headrest contact, the data indicate that head-driven loading may be influencing cervical spine response. It is therefore hypothesized that the neck undergoes a distinct bending mode under these conditions, analogous to buckling behavior observed in axially loaded beams. This phenomenon is evident in acceleration responses but not in displacement metrics. Future studies incorporating angular rate sensors at individual vertebral levels are recommended to further characterize the underlying neck loading mechanisms. It is important to acknowledge that the T1-clavicle rig used to acquire T1 data from volunteers has inherent limitations and may not fully capture the true kinematic response of the volunteer, while ATD measurements have minute uncertainty.

The overall BioRank for the EvaRID-50F is 1.11 (0.97 excluding Pelvis X Displacement), corresponding to a Good biofidelity classification. All evaluated parameters remained below the acceptance threshold of 2.0, except for Pelvis X Displacement, as discussed subsequently. No temporal discrepancies were observed between ATD and volunteer responses, and no design modifications were required to achieve the reported performance. All four ATDs were evaluated under both test conditions, with the most recent datasets presented herein. Biofidelity testing was conducted with improved efficiency, benefiting from enhanced scheduling flexibility and streamlined communication. Furthermore, all ATDs demonstrated robust durability, with no structural or functional failures observed during testing.

Pelvis X displacement represents the most significant discrepancy between volunteer and ATD responses, despite being a nominally biofidelic parameter. The observed 25 mm difference cannot be attributed to any controlled variables within the present study. The ATD measures pelvic motion directly using either the pelvis flag or H-point tool, both of which yield consistent results. In the volunteer configuration, the pelvis is observed to contact the lowest seat panel, Figure 1 in [1], and the EvaRID-50F positioning procedure ensures an identical initial condition, thereby excluding initial positioning as a source of discrepancy [1]. A rigid support bar located immediately behind the pelvis panel [4] has only 78.6 mm of available rearward displacement, which contradicts the extent of motion suggested by the volunteer corridor. Furthermore, neither the ATD nor volunteer datasets exhibit characteristic signatures of panel-bottoming, such as abrupt plateaus or truncation, instead displaying smooth temporal responses. The extrapolation method used in volunteer testing, which derives pelvis motion from tracked femoral markers relative to the trochanter, is expected to provide a reasonable approximation of pelvic motion, indicating that computational methodology is unlikely to be the primary source of error [1]. Additionally, [4] published Pelvis X displacement of approximately 70 mm with 50th percentile male volunteers under a similar sled pulse, but instead of the trochanter calculation method, displacement was measured through a pelvis rig mounted near the iliac spine. The pelvis panel X displacement of the male volunteers was 30 mm without plateaus or truncation, which aligns with the EvaRID-50F data rather than the female volunteer data. The leading hypothesis is that the tracked markers exhibit an approximate 25 mm displacement due to soft tissue motion, thereby inflating the inferred pelvis displacement. A secondary hypothesis is that leg lift during sled acceleration alters the kinematic relationship used for extrapolation; however, this is considered unlikely given the low acceleration levels and short duration (~125 ms) to peak motion. Evaluation of these hypotheses remains beyond the scope of the present study. Collectively, the evidence indicates that the volunteer and ATD measurement techniques may not quantify the same physical parameter, thereby undermining direct biofidelity comparison for Pelvis X displacement. Due to this uncertainty, BioRank values are reported both including and excluding this parameter.

For biofidelity parameters evaluated with a 500 ms duration, both volunteer and ATD responses exhibit pronounced rebound variability, indicative of chaotic post-impact motion. Head and T1 responses in the volunteer dataset display substantially broadened corridors relative to peak magnitudes, a trend similarly observed in the ATD data. In contrast, Pelvis X Displacement does not exhibit comparable corridor expansion. The oscillatory behavior observed in the volunteer responses suggests active neuromuscular engagement, including muscle bracing and adaptation, which cannot be replicated by the ATD. Consequently, restricting the BioRank evaluation window to 0–300 ms is justified, as it isolates the primary impact phase and avoids confounding influences from rebound dynamics. Both 10 cm and 15 cm headrest distances serve different but equally important functions. 10 cm test condition is more representative of ATD use cases during regulation testing of car seats, while the 15 cm test condition allows more neck motion and rotation to compare to human performance.

V. CONCLUSION

The EvaRID-50F was evaluated using four ATDs under two test conditions, yielding an overall BioRank of 1.11 (0.97 excluding Pelvis X displacement), corresponding to a "Good" biofidelity classification. The Pelvis X Displacement parameter requires further investigation to resolve the significant discrepancy observed between ATD and volunteer responses. The EvaRID-50F was directly derived from the CAE v1.0 EvaRID, with usability-focused modifications that did not alter performance-critical characteristics. A replicated Chalmers seat was developed and validated, providing a consistent platform for biofidelity evaluation. Future work should include repeatability and reproducibility studies using the ENCAP rear impact pulse, as well as further investigation into parameters governing head and neck kinematics during impact events. A comparison study to the CAE EvaRID model will expand the confidence in both the physical and the virtual EvaRID's. The EvaRID-50F is positioned for potential regulatory adoption and is expected to contribute to improved whiplash injury mitigation for female occupants worldwide.

VI. ACKNOWLEDGEMENTS

The authors would like to thank Dr. Anna Carlsson, Dr. Astrid Linder, and Dr. Mats Svensson for the knowledge of the sled tests performed at Chalmers University. Thank you also for allowing the authors to borrow the Chalmers seat used in the testing so that a replica could be made.

AI Use Disclosure: M365 Copilot, based on GPT-5 chat model, were used to support language editing. All scientific content, interpretations, and conclusions were developed, reviewed, and validated by the authors, who take full responsibility for the accuracy and integrity of the work.

VII. REFERENCES

[1] Carlsson, A., Hourion, S., et al. (2021) Dynamic Responses of Female Volunteers in Rear Impact Sled Tests at Two Head Restraint Distances. Frontiers in Bioengineering and Biotechnology, 9:684003.

[2] Linder, A. "ADSEAT Develops Important New Occupant Model for Car Safety", https://www.adseat.eu/files/pages/23/adseat-final-newsletter-18apr13.pdf. [2026 April 3]

[3] Carlsson, A. Chang, F., et al. (2012) EvaRID – A 50th Percentile Female Rear Impact Finite Element Dummy Model. *IRCOBI*, 2012, Dublin, Ireland.

[4] Davidsson, J., Deutscher, C., Hell, W., Linder, A., Lövsund, P., Svensson, M. Y. (1998) Human Volunteer Kinematics in Rear-End Sled Collisions. *IRCOBI*, 1998, Gothenburg, Sweden.

[5] (2021) Mutual Resolution Addendum 1. UNECE, 2021, Geneva, Switzerland.

[6] Carlsson, A., Davidsson, J., Linder, A., Svensson, M. Y. (2021) Design and Evaluation of the Initial 50th Percentile Female Prototype Rear Impact Dummy, BioRID P50F – Indication for the Need of an Additional Dummy Size. Frontiers in Bioengineering and Biotechnology, 9:687058.

[7] Jobin, J., Klug, C., Kranjec, M., Svenning, E., Iraeus, J., (2022) Hello, world! VIVA+: A human body model lineup to evaluate sex-differences in crash protection. Frontiers in Bioengineering and Biotechnology, 10:918904

[8] Rhule, H., Sticklin, J., Donnelly, B., Moorhouse, K. (2018) Improvements to NHTSA's Biofidelity Ranking System and Application to the Evaluation of the THOR 5th Female Dummy. Proceedings of the IRCOBI Conference, 12–14 September 2018, Athens, Greece.

[9] Hagedorn, A., Stammen, J., et al. (2022) Biofidelity evaluation of THOR-50M in rear-facing seating configurations using an updated biofidelity ranking system. SAE International Journal of Transportation Safety, 10(2): pp. 291–376. https://www.jstor.org/stable/27215865.

VIII. APPENDIX A

Table 4

CHANNEL NAME	PART #	FILTER CLASS	USED FOR BIOFIDELITY TESTING	BIORANKED
SLED ACCELERATION	7264C	CFC60	OUTSIDE ATD	
HEAD X DISPLACEMENT	HIGH-SPEED CAMERA	CFC60	OUTSIDE ATD	X
HEAD Z DISPLACEMENT	HIGH-SPEED CAMERA	CFC60	OUTSIDE ATD	X
HEAD Y ANGULAR DISPLACEMENT	HIGH-SPEED CAMERA	CFC60	OUTSIDE ATD	X
T1 X DISPLACEMENT	HIGH-SPEED CAMERA	CFC60	OUTSIDE ATD	X
T1 Z DISPLACEMENT	HIGH-SPEED CAMERA	CFC60	OUTSIDE ATD	X
T1 Y ANGULAR DISPLACEMENT	HIGH-SPEED CAMERA	CFC60	OUTSIDE ATD	X
HEAD RELATIVE TO T1 X DISPLACEMENT	CALCULATED	CFC60	OUTSIDE ATD	X
HEAD RELATIVE TO T1 Y ANGULAR DISP	CALCULATED	CFC60	OUTSIDE ATD	X
PELVIS X DISPLACEMENT	HIGH-SPEED CAMERA	CFC60	OUTSIDE ATD	X
HEAD CG ACCELERATION X	7264H	CFC1000	INSIDE ATD	X
HEAD CG ACCELERATION Y	7264H	CFC1000		
HEAD CG ACCELERATION Z	7264H	CFC1000	INSIDE ATD	X
HEAD CG ANGULAR RATE X	IT-600	CFC180		
HEAD CG ANGULAR RATE Y	IT-600	CFC180	INSIDE ATD	
HEAD CG ANGULAR RATE Z	IT-600	CFC180		
3X SKULL CAP LC, BIORID, FX	6350JD6I4	CFC1000	INSIDE ATD	
3X SKULL CAP LC, BIORID, FY	6350JD6I4	CFC1000	INSIDE ATD	
3X SKULL CAP LC, BIORID, FZ	6350JD6I4	CFC1000	INSIDE ATD	
SKULL CAP CONTACT SWITCH, EVARID	305-1120	N/A	INSIDE ATD	
6X UPPER NECK LOAD CELL, EVARID, FX	IH-13570J	CFC1000	INSIDE ATD	
6X UPPER NECK LOAD CELL, EVARID, FY	IH-13570J	CFC1000	INSIDE ATD	
6X UPPER NECK LOAD CELL, EVARID, FZ	IH-13570J	CFC1000	INSIDE ATD	
6X UPPER NECK LOAD CELL, EVARID, MX	IH-13570J	CFC600	INSIDE ATD	
6X UPPER NECK LOAD CELL, EVARID, MY	IH-13570J	CFC600	INSIDE ATD	
6X UPPER NECK LOAD CELL, EVARID, MZ	IH-13570J	CFC600	INSIDE ATD	
HEAD DUAL AXIS TILT SENSOR	IES-1402	N/A	INSIDE ATD	
T1 LEFT ACCELERATION X	7264H	CFC60	INSIDE ATD	X
T1 LEFT ACCELERATION Z	7264H	CFC60	INSIDE ATD	X
T1 RIGHT ACCELERATION X	7264H	CFC60	INSIDE ATD	X
T1 RIGHT ACCELERATION Z	7264H	CFC60	INSIDE ATD	X
T1 RIGHT ANGULAR RATE Y	IT-600	CFC180	INSIDE ATD	
3X T1 LOAD CELL, EVARID, FX	IH-13580J	CFC1000	INSIDE ATD	
3X T1 LOAD CELL, EVARID, FZ	IH-13580J	CFC1000	INSIDE ATD	
3X T1 LOAD CELL, EVARID, MY	IH-13580J	CFC600	INSIDE ATD	
T1 DUAL AXIS TILT SENSOR	IES-1402	N/A	INSIDE ATD	
T8 LEFT ACCELERATION X	7264H	CFC180	INSIDE ATD	
T8 LEFT ACCELERATION Z	7264H	CFC180	INSIDE ATD	
T8 LEFT ANGULAR RATE Y	IT-600	CFC60	INSIDE ATD	
T8 RIGHT ACCELERATION X	7264H	CFC180		
T8 RIGHT ACCELERATION Z	7264H	CFC180		
T8 RIGHT ANGULAR RATE Y	IT-600	CFC60		
T8 DUAL AXIS TILT SENSOR	IES-1402	N/A	INSIDE ATD	
L1 LEFT ACCELERATION X	7264H	CFC180	INSIDE ATD	
L1 LEFT ACCELERATION Z	7264H	CFC180	INSIDE ATD	

L1 LEFT ANGULAR RATE Y	IT-600	CFC60	INSIDE ATD
L1 DUAL AXIS TILT SENSOR	IES-1402	N/A	INSIDE ATD
6X L5 SEGMENT LOAD CELL, EVARID, FX	IH-13640J	CFC600	INSIDE ATD
6X L5 SEGMENT LOAD CELL, EVARID, FY	IH-13640J	CFC600	INSIDE ATD
6X L5 SEGMENT LOAD CELL, EVARID, FZ	IH-13640J	CFC600	INSIDE ATD
6X L5 SEGMENT LOAD CELL, EVARID, MX	IH-13640J	CFC600	INSIDE ATD
6X L5 SEGMENT LOAD CELL, EVARID, MY	IH-13640J	CFC600	INSIDE ATD
6X L5 SEGMENT LOAD CELL, EVARID, MZ	IH-13640J	CFC600	INSIDE ATD
Ø.850 SKULL SPRING LOAD CELL, ANTERIOR	10386JDI4-250	CFC600	
Ø.850 SKULL SPRING LOAD CELL, POSTERIOR	10386JDI4-250	CFC600	
PELVIS CG ACCELERATION X	7264H	CFC180	INSIDE ATD
PELVIS CG ACCELERATION Y	7264H	CFC180	
PELVIS CG ACCELERATION Z	7264H	CFC180	INSIDE ATD
PELVIS CG ANGULAR RATE X	IT-600	CFC60	
PELVIS CG ANGULAR RATE Y	IT-600	CFC60	INSIDE ATD
PELVIS CG ANGULAR RATE Z	IT-600	CFC60	
PELVIS DUAL AXIS TILT SENSOR	IES-1402	N/A	INSIDE ATD
TOTAL DAS CHANNELS	47		36
TOTAL NON-DAS CHANNELS	5		5

IX. APPENDIX B

Test Num	1	2	3	4	5	6	7	8	9	10	11	12
File Name for **15cm** Headrest Distance	EvaRID-2_FF8679_Test-3	EvaRID-2_FF8679_Test-6	EvaRID-2_FF8679_Test-7	EvaRID-3_FF8680_Test-2	EvaRID-3_FF8680_Test-3	EvaRID-3_FF8680_Test-4	EvaRID-1_FF8678_Test-8 PostDuro	EvaRID-1_FF8678_Test-9 PostDuro	EvaRID-1_FF8678_Test-10 PostDuro	EvaRID-4_FJ3212_Test-4	EvaRID-4_FJ3212_Test-5	EvaRID-4_FJ3212_Test-6
Head x-displacement	0.88	0.84	0.9	0.95	0.92	0.89	0.74	0.7	0.78	0.89	0.99	0.79
T1 x-displacement	0.87	0.96	0.74	0.77	1.33	0.97	1.12	1.08	0.96	0.84	1.03	0.72
Head rel T1 x-displ.	1.93	1.64	1.85	1.99	1.77	1.91	1.9	1.94	1.99	1.07	1.01	1.02
Head Angular Displacement	0.55	0.63	0.47	0.68	0.77	0.68	0.85	0.75	0.71	0.87	0.98	0.89
T1 Angular Displacement	0.44	0.46	0.5	0.39	0.76	0.63	1.03	0.85	1.2	0.67	0.79	0.78
Head rel T1_Angle	0.49	0.51	0.47	0.76	0.51	0.56	0.64	0.55	0.49	1.08	1.02	1.09
Head minus T1 Rotation	0.52	0.54	0.53	0.8	0.54	0.59	0.67	0.58	0.5	0.77	0.79	0.74
Head X Accel	1.22	1.24	1.31	1.07	1.14	1.1	1.25	1.22	1.26	1.7	1.7	1.68
T1 Left X Accel	1.45	1.65	1.6	1.45	1.57	1.53	1.77	1.74	1.86	1.58	1.43	1.46
T1 Right X Accel	1.4	1.58	1.59	1.37	1.58	1.46	1.79	1.73	1.9	1.55	1.34	1.43
Head Z Accel	0.53	0.6	0.55	0.54	0.61	0.61	0.65	0.65	0.68	0.75	0.83	0.7
T1 Left Z Accel	0.94	0.94	0.85	1.13	1.01	1.06	1.06	0.9	0.93	1.26	1.26	1.19
T1 Right Z Accel	0.87	0.9	0.83	1.12	1	1.07	1.05	0.92	0.9	1.27	1.27	1.18
Pelvis x-displacement							2.52	2.5	2.16	2.9	2.93	2.59
H-point x-displacement							2.63	2.75	2.38	2.75	2.7	2.49

Test Num	1	2	3	4	5	6	7	8	9	10	11	12
File Name for **10cm** Headrest Distance	EvaRID-2_FF8679_Test-1	EvaRID-2_FF8679_Test-2	EvaRID-2_FF8679_Test-3	EvaRID-3_FF8680_Test-3	EvaRID-3_FF8680_Test-4	EvaRID-3_FF8680_Test-5	EvaRID-1_FF8678_Test-6	EvaRID-1_FF8678_Test-7	EvaRID-1_FF8678_Test-8	EvaRID-4_FJ3212_Test-4	EvaRID-4_FJ3212_Test-5	EvaRID-4_FJ3212_Test-6
Head x-displacement	0.53	0.48	0.58	0.83	0.86	0.92	0.55	1	0.57	1.05	1.02	1.08
T1 x-displacement	0.7	1.11	0.83	0.59	0.58	0.52	1.15	0.7	1.18	0.72	0.55	0.65
Head rel T1 x-displ.	0.48	0.57	0.57	0.91	0.87	1.06	0.95	1.09	1.05	0.88	0.79	0.93
Head Angular Displacement	0.27	0.28	0.29	0.25	0.24	0.23	0.23	0.24	0.19	0.35	0.29	0.37
T1 Angular Displacement	1.9	1.7	1.83	1.95	1.9	1.72	1.89	1.68	1.58	2	1.91	1.82
Head rel T1_Angle	0.42	0.43	0.41	0.45	0.4	0.46	0.72	0.53	0.54	0.42	0.42	0.43
Head minus T1 Rotation	0.42	0.44	0.42	0.46	0.4	0.45	0.67	0.5	0.51	0.33	0.34	0.32
Head X Accel	0.86	0.77	0.88	1.09	1.08	1.12	1.16	1.34	0.92	1.37	1.34	1.5
T1 Left X Accel	1.11	1.12	1.11	0.95	1.07	0.95	0.92	1.13	1.02	1.1	0.9	1.12
T1 Right X Accel	1.08	1.05	1.07	0.87	1	0.89	0.93	1.22	1.03	1.09	0.95	1.12
Head Z Accel	0.68	0.65	0.68	0.74	0.75	0.71	0.77	0.69	0.68	0.77	0.75	0.84
T1 Left Z Accel	1.16	1.15	1.13	1.23	1.27	1.32	1.21	1.26	1.34	1.27	1.28	1.28
T1 Right Z Accel	1.1	1.04	1.08	1.19	1.27	1.29	1.15	1.17	1.26	1.27	1.3	1.32
Pelvis x-displacement							2.7	2.61	2.74	2.47	2.55	2.72
H-point x-displacement							2.83	2.76	2.93	2.31	2.42	2.67